

**Bulletin 54
(Part 3 of 3 Parts)**

Reprinted From

**THE
SHOCK AND VIBRATION
BULLETIN**

**Part 3
Structural Dynamics,
Machinery Dynamics and
Vibration Problems**

JUNE 1984

**A Publication of
THE SHOCK AND VIBRATION
INFORMATION CENTER
Naval Research Laboratory, Washington, D.C.**



**Office of
The Under Secretary of Defense
for Research and Engineering**

Approved for public release; distribution unlimited.

VIBRATIONAL LOADING MECHANISM OF UNITIZED CORRUGATED CONTAINERS
WITH CUSHIONS AND NON-LOAD-BEARING CONTENTS

Thomas J. Urbanik, Research General Engineer
Forest Products Laboratory,* Forest Service
U.S. Department, of Agriculture

The use of hardwood and recycled fiber will no doubt increase as specifications for corrugated fiberboard containers change from material to performance standards. This report shows another way to accelerate this use by reducing the strength requirements of containers shipped in unitized loads. The rate of container deformation with top loading and the compliance of internal packing material or cushions are newly identified variables governing the compression of bottom containers.

Unitized containers need strength beyond the warehouse stacking requirements to support dynamic loads during shipping. The spring rates of top-loaded containers and internal cushions amplify the weight force of a unitized load during transportation. The progressive deformation with top-loading of corrugated Containers causes increasingly higher spring rates with a subsequent effect on dynamic loads. Cushions or internal packing provide a natural ability to absorb vibrations to a degree, depending on their spring rates relative to the containers'.

Over-the-road shipping vibrations encompass the natural frequencies of most unitized loads and dynamically load the bottom containers. A worst case assessment calculates the maximum load on the bottom tier, expected during truck transportation. The cushion-to-container spring ratio and the rate of increasing container spring rates with top-loading are the primary variables determining dynamic loads.

NOMENCLATURE

C_t	Total compressive loading factor	K_n	Container spring rate in tier n
c_{ci}	Critical damping coefficient of element i	K_p	Container spring rate with top load P
c_i	Damping coefficient of element i	K_w	Container spring rate with top load W
[D]	Damping matrix	K_1	Container spring rate with unit top load
$[D_{ij}]$	Partition of damping matrix	k_i	Stiffness coefficient of element i
F	Cushion-to-container spring ratio	[M]	Mass matrix
f	Natural frequency factor	m	Unit mass
f_1	Lowest natural frequency factor	m_i	Mass of element i
G	Gravitational constant	N	Number of mass elements
[I]	Identity matrix	n	Tier number
i	Element number in spring-mass model	P	Top load
j	Imaginary unit	P_d	Dynamic compressive load
K_c	Cushion spring rate	[R]	A matrix of stiffness coefficients
K_N	Bottom container spring rate	$[\sqrt{R}]$	A matrix of stiffness coefficients
		r	Exponent in spring rate formula
		[S]	Stiffness matrix
		$\{S_c\}$	Condensed stiffness matrix
		$\{S_{ij}\}$	Partition of stiffness matrix
		W	Unit weight per container
		{X}	Response vector

* Maintained at Madison, Wis., in cooperation with the University of Wisconsin.

x_{N+1}	Displacement of element N+1
\ddot{x}_{N+1}	Acceleration of element N+1
$\{Y\}$	Disturbance vector
$\{Y'\}$	Partition of disturbance vector
Y	Displacement disturbance
\ddot{Y}	Acceleration disturbance
ρ	Damping ratio
ω	Natural frequency
ω_1	Lowest natural frequency
$\{0\}$	Zero matrix
$\{0,0\}$	Zero vector

INTRODUCTION

One problem with designing corrugated fiberboard containers is determining an adequate load carrying ability. The top-to-bottom compressive strength measured in a laboratory test is the upper limit of strength expected under only the most favorable conditions. The problem of comparing this strength to the anticipated dynamic load becomes particularly relevant when containers are shipped in unitized loads. While the additive weight of the upper containers is obvious, it is not always apparent how to treat the effects of over-the-road vibrations.

Unitized containers need extra strength beyond the warehouse stacking requirements to support dynamic loads during shipping. One of the surest methods for assessing adequate strength is the ASTM Vibration Test [1]. However, being empirical, its application is a trial and error search for a unitized load that survives the test.

An analysis can speed up the search, and one of the earliest is that by Godshall [2]. Godshall treated corrugated containers as spring-mass systems, and determined which characteristics would predict their response to transportation vibrations. He used repeated loading compression tests to measure the spring rates of top-loaded containers. Later vibration experiments by Godshall [3] confirmed the effectiveness of these tests. A primary finding was that corrugated-container systems will likely resonate during shipping with destructive compressive forces limited primarily by material damping, empirically determined to be 0.115 times the critical damping value.

With machines where changing damping is impracticable, engineers have attached vibration absorbers to stabilize their motion. Analogously, it makes sense that cushions within containers can reduce unit load vibrations. Hatae [4] gives a comprehensive treatment of the mechanics of package cushions. Godshall [5] applied these concepts to corrugated pads and compared spring rates determined from repeated loading tests with values calculated from resonant frequencies determined in vibration tests. The vibration test is more

accurate; especially when the loading condition between a product and cushion may be uncertain.

While Godshall studied only single degree of freedom systems, my earlier work [6,7] proposed a new theory and a computer program for multiple degree of freedom systems. Calculations with representative spring rates and damping characteristics of corrugated containers explained why disturbances at only the lowest of multiple natural frequencies inherent to a unitized load cause problems. One example trial of my computer program evaluated a unitizing arrangement in a theoretical shipping environment for dynamic compression of the bottom containers.

The investigation by Ostrem and Godshall [8] quantified the actual shipping environment for unitized loads. Figure 7 in their report summarizes the envelope of truck vibrations and suggests that calculating the response of unitized loads for a 0.5 G acceleration disturbance predicts the hazards associated with this mode of shipping.

This previous research thus established the following principles leading to this study: (1) Repeated loading tests predict the spring rates of corrugated containers; (2) spring rates of cushions are determinable from vibration tests; (3) corrugated fiberboard systems are damped at about 0.115 times the critical damping value; (4) the first natural frequency is of primary concern, and the truck transportation environment normally excites that frequency; and (5) vibration disturbances in trucks are typically about 0.5 G in magnitude.

OBJECTIVE AND SCOPE

The objective of this report is to explain how the spring rates of cushions and containers amplify the compressive weight force of a unitized load during truck transportation. This study starts by measuring spring rates of combinations of corrugated containers and plastic bottles. The experiments lead to a formula for predicting the spring rates of containers in different tiers of a stack. A theory proposes the behavior of a unitized load having definable ratios among its components' spring rates. The spring rates of cushions enter the theory as a means of reducing the dynamic response of a stack. A spring-mass model of a unitized load guides the theory through a matrix analysis for which a set of dimensionless parameters greatly reduces the number of variables.

While transportation vibrations can disarrange a unitized load or resonate the contents, the primary mode of damage considered in this report is compression of the bottom containers. The theory treats a specific type of package wherein the innermost contents carry no load, although the interior package might share the load with the box. Moreover, these contents

act like lumped masses suspended on cushions resulting from actual cushions within the boxes, the compliance of interior packages, or when the contents are soft, their own compliance.

The general principles of vibration isolation discussed in [9] indicate the significance of material damping. Although arbitrary cushioning materials may encompass wide variations in damping characteristics, this study considers only one damping ratio typical of corrugated fiberboard. An application of the theory calculates compressive loads for combinations of spring rates and numbers of unitized tiers. The results suggest ways to reduce the strength requirement of boxes used in unitized loads.

TEST MATERIAL AND PROCEDURE

A repeated loading test top-loads a container to an equilibrium value equal to the static load. It normally supports then repeatedly raises and lowers the load to simulate vibrations and establish a linear section of the load deformation trace. A series of repeated loading tests for this study measured the spring rates of corrugated Containers and plastic water bottles. The bottles were nominal 1-gallon, commercial plastic bottles for distributing distilled water. The boxes were nominal 200-pound C-flute commercial, regular-slotted containers intended for the bottles.

To test the effect of load sharing between the bottles and the box, 16 test units were separated into four arrangements. Units 1-9 were tested in the normal arrangement of a box containing six bottles filled with water. Tests of units 10-13 used a box with six sand filled bottles having cut-down tops. Each bottle contained 3.8 kg of sand. This arrangement concentrated the top load in the box while providing the normal lateral pressure.

The reverse arrangement whereby the bottles carried all of the load was used for testing units 14 and 15. The midsection about the perimeter of each box was cut away and the box contained six water-filled bottles. Unit 16 consisted of six water-filled bottles with no box.

To test the effect of environmental conditions, the tests were conducted at three different temperatures and relative humidities (RH). Units 1-3 and 16 were tested at 73°F and 50 percent RH; units 4-6, at 80°F and 30 percent RH; and units 7-15, at 80°F and 90 percent RH. Container preparation followed the normal preconditioning in a dry environment according to ASTM D 685-73 [10] with subsequent conditioning at the prescribed testing environment. Conditioning times were long enough to ensure an equilibrium moisture content of the material.

A check was made for vibrational work hardening. While other units were unused prior to compression tests, units 10-12 consisted of containers used in previous vibration tests performed at 30 and 90 percent RH for another study.

Each unit underwent 16 repeated loading tests. Each test first compressed the container between two parallel platens at a rate of 42.3 μm/s up to an equilibrium load (EL) followed by repeatedly raising and lowering the load with an amplitude determined as a percentage of the EL. The 16 tests consisted of all combinations of 4 EL's and 4 percentages of EL.

Equilibrium loads of 25, 50, 75, and 100 kg duplicated the static top load per container due to the upper four tiers of a stack. Repeated loading and unloading between amplitudes of 25, 50, 75, and 100 percent of each EL simulated different vibration magnitudes.

Load was measured with an electronic transducer attached to the bottom platen and deformation with a drum recorder whose rotation was mechanically proportional to the displacement of the upper platen. Five cycles of loading were enough to produce a repeating load deformation trace.

DATA AND ANALYSIS

The spring rate of a container equals the slope of a tangent drawn at the EL to the trace produced by the final increasing load. The spring rate data appear in Table I.

Spring rates of the containers in units 1-15 follow the empirical formula

$$K_p = K_w (P/W)^r \quad (1)$$

P is the EL and K_p is the spring rate at that load. W is a reference load and K_w the corresponding spring rate. r is an empirical constant. A modified formula represents conditions in a unit load by considering only values of P and K_p identified with each tier. Let the reference load, W, equal the unit weight per container and number the tiers 1, 2, ... N as shown in Figure 1 beginning with the second tier from the top. If $n = P/W$, equation (1) reduces to

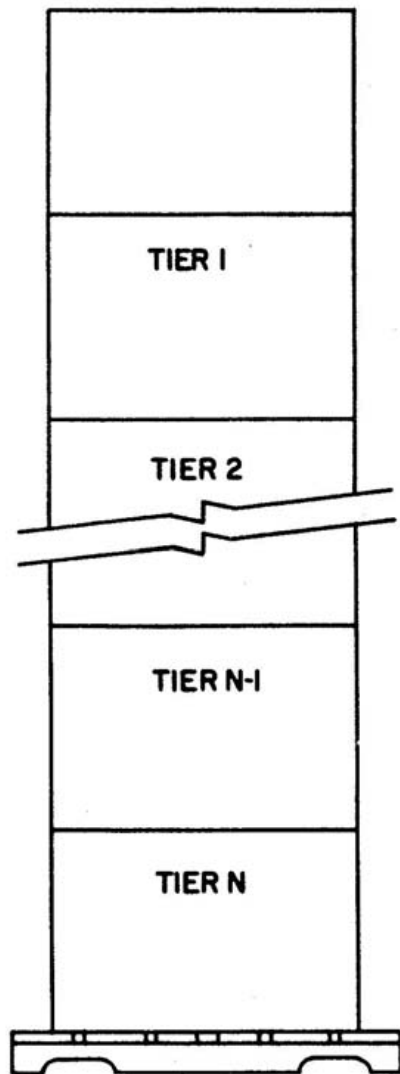
$$K_n = K_1 n^r ; \quad n = 1, N \quad (2)$$

where K_n is the spring rate at tier n.

Table 1.--Container spring rates

		Container arrangement and unit number															
Repeated loading amplitude	Equilibrium load	Box with six water-filled bottles									Box with six sand-filled bottles having cut-down tops				Box with cut-away mid-section and six water-filled bottles		Six water-filled bottles with no box
		73°F, 50% R.H.			80°F, 30% R.H.			80°F, 90% R.H.			80°F, 90% R.H.						73°F, 50% R.H.
		1	2	3	4	5	6	7	8	9	10 ^{1/}	11 ^{1/}	12 ^{1/}	13			16
															14	15	
Pct of EL	kg	----- kN/m -----															
25	25	376	214	339	341	350	362	196	269	178	333	208	239	210	214	201	584
	50	500	362	600	501	477	420	568	618	466	584	412	447	477	256	226	618
	75	778	725	750	724	750	656	913	995	808	1,070	1,170	890	914	404	362	656
	100	955	913	913	955	913	808	955	1,050	913	1,690	1,110	1,750	1,630	553	512	636
50	25	202	194	339	258	277	244	291	328	178	256	191	223	196	194	178	512
	50	477	362	525	438	429	396	584	656	477	664	477	429	411	253	242	568
	75	677	656	725	618	538	618	725	913	750	1,110	913	913	840	388	323	618
	100	808	808	840	750	677	700	875	1,105	875	1,880	808	1,280	1,500	447	500	538
75	25	184	178	300	242	234	223	202	280	142	210	170	187	196	166	163	466
	50	457	339	477	382	382	362	500	538	368	553	362	389	333	259	219	525
	75	584	584	636	500	500	553	618	808	584	955	761	778	700	344	284	525
	100	700	725	700	636	600	618	700	954	636	1,400	--	1,030	1,170	375	382	438
100	25	156	159	309	228	223	215	187	244	137	187	116	160	163	149	150	429
	50	404	298	447	389	350	307	412	429	328	466	305	313	291	193	189	525
	75	553	584	558	457	457	501	457	656	447	750	636	636	584	246	242	500
	100	600	636	648	553	512	583	584	700	500	1,050	--	--	914	313	339	368

1/ Boxes were used in vibration tests performed at 30% and 90% R.H. prior to compression testing.



ML83 5399

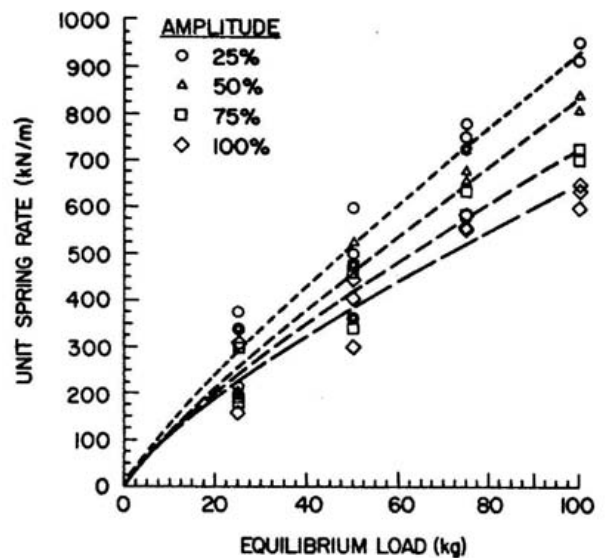
Figure 1.--Representation of a unitized load. The tiers are numbered to match the static loading condition.

Equation (2) reduces the measured spring rates K_1 , K_2 , K_3 , and K_4 to predicted parameters in terms of K_1 and r for each repeated loading amplitude of each group of data. The values of K_1 and r fitting the data appear in Table 11.

Table 11.--Parameters K_1 and r determined from repeated loading data

Repeated Loading amplitude	Unit number					
	1-3	4-6	7-9	10-12	13	14,15
<u>Pct of EL</u>						
	K_1 (kN/m)					
25	291	307	282	202	142	159
50	255	258	305	228	120	160
75	239	233	250	173	115	160
100	226	224	219	134	114	136
	r					
25	.838	.757	.937	1.46	1.74	.838
50	.856	.734	.840	1.28	1.81	.759
75	.801	.710	.835	1.41	1.66	.618
100	.765	.655	.746	1.48	1.49	.620

Figures 2 and 3 show some representative plots of the data and average characteristics. As evidenced in Figure 2, higher repeated loading amplitudes cause lower spring rates. Table 11, however, suggests that the effect of amplitude on the predicted r 's is not serious.



ML83 5401

Figure 2.--Spring rate versus equilibrium load for top-loaded corrugated containers and plastic bottles of units 1-3. The points represent the data. The curves fit equation (1) to data obtained with 25, 50, 75, and 100 percent repeated loading amplitudes.

Figure 3 shows the effects of the different arrangements, environments, and prior use. A comparison among units 1-3, 4-6, and 7-9 shows the combined effects of temperature and humidity. The contribution of load sharing by the bottles becomes evident by comparing units 7-9 with unit 13 and units 14, 15. Work hardening permanently deforms the paperboard material and increases the spring rates of lightly loaded containers. Comparing units 10-12 with unit 13 shows this effect.

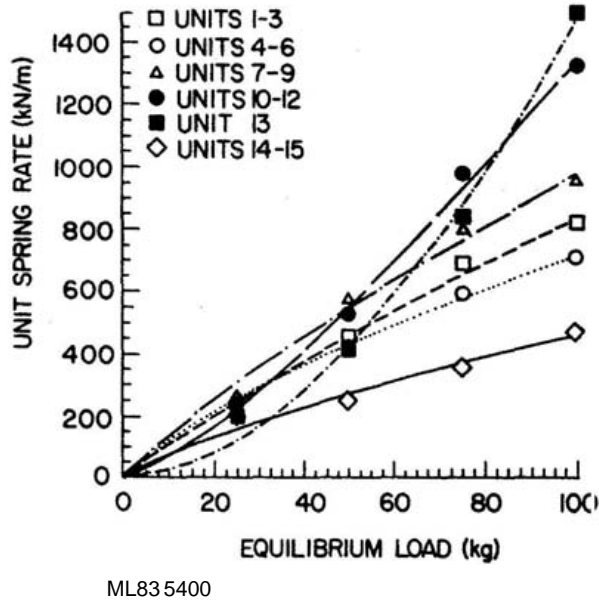


Figure 3.--Spring rate versus equilibrium load with a repeated loading amplitude of 50 percent of the equilibrium load. The points represent the average data. The curves fit equation (1) to the data.

A series of repeated loading tests can be abbreviated by testing only two containers. Determine spring rates, K_1 and K_N for the second and bottom tiers in a unit load and calculate r from

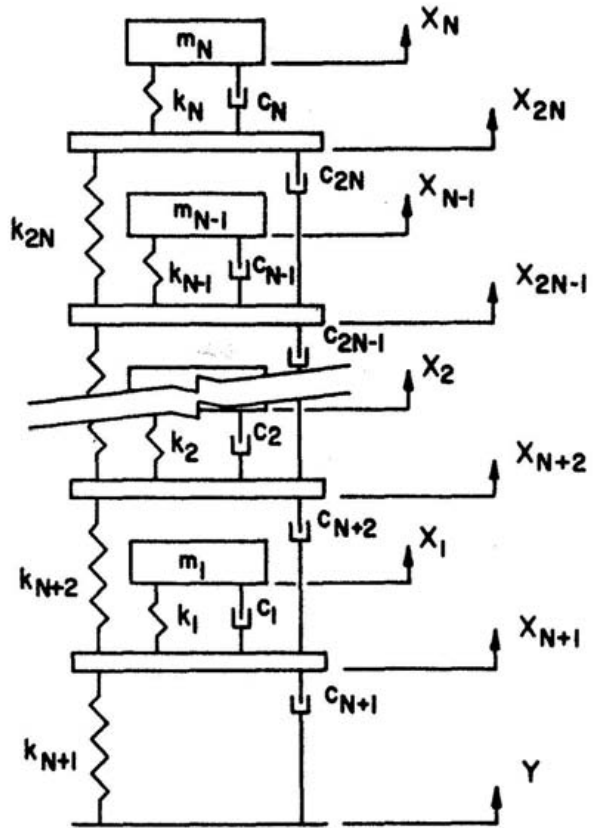
$$r = \frac{\ln (K_N/K_1)}{\ln N} \quad (3)$$

Of course extra tests check the variability.

THEORY

The diagram in Figure 4 represents a unitized load with cushioned, non-load-bearing masses. A model with N masses has $2N$ degrees of freedom corresponding to a unit load with $N + 1$ tiers. My step by step analysis of a similar model appears in [6,7]. This theory

follows the same steps where, after associating equations of equilibrium with the degrees of freedom, it arranges the equations for a matrix solution. To simplify the analysis the theory introduces six dimensionless parameters, of which N and r have already been mentioned.



ML83 5398

Figure 4.--Representation of a unitized load as a spring-mass system. The degrees of freedom are numbered for calculating the dynamic loading condition.

The weight of the contents of each container is lumped into a mass m . All masses being equal gives

$$m_i = m = W/G \quad ; \quad i = 1, N \quad (4)$$

The interior springs represent cushions and remain equal provided the container compression does not interfere with the mass vibration. Call the spring rate of the cushions K_c and let the dimensionless parameter F be the cushion-to-container spring ratio.

$$F = K_c / K_1 \quad (5)$$

The corresponding stiffness values become

$$k_i = FK_1 \quad ; \quad i = 1, N \quad (6)$$

The outer springs follow the behavior of top-loaded containers becoming increasingly stiffer progressing down the stack. Starting with element k_{2N} identified with tier 1, and being careful to note the difference between tier numbers in Figure 1 and spring numbers in Figure 4, the stiffness values are

$$k_{2N+1-i} = K_1 i^r \quad ; \quad i = 1, N \quad (7)$$

The assumption of viscous damping explained Godshall's data [3] reasonably well and is extended here to a unitized load. If the critical damping associated with each dashpot is

$$c_{ci} = 2 \sqrt{mk_i} \quad ; \quad i = 1, 2N \quad (8)$$

and all elements have equal damping ratios, ρ , they take on damping values given by

$$c_i = \rho c_{ci} = 2 \rho \sqrt{mk_i} \quad ; \quad i = 1, 2N \quad (9)$$

The mass matrix [M] of size $2N \times 2N$ is constructed from the identity submatrix [I] and the zero submatrix [0] both of size $N \times N$.

$$[M] = m \begin{bmatrix} I & \vdots & 0 \\ 0 & \vdots & 0 \end{bmatrix} \quad (10)$$

The stiffness matrix [S] of size $2N \times 2N$ is partitioned into submatrices $[S_{11}]$, $[S_{12}]$, $[S_{21}]$, and $[S_{22}]$ all of size $N \times N$. The partitions are constructed according to equations

$$\left. \begin{aligned} [S_{11}] &= K_1 F [I] \\ [S_{12}] &= [S_{21}] = -[S_{11}] \\ [S_{22}] &= K_1 [R] \end{aligned} \right\} \quad (11)$$

where [R] appears in Table 111. The complete form of [S] is finally

$$[S] = \begin{bmatrix} S_{11} & \vdots & S_{12} \\ \vdots & \ddots & \vdots \\ S_{21} & \vdots & S_{22} \end{bmatrix} \quad (12)$$

The damping matrix [D] is partitioned as [S] was according to

$$[D] = \begin{bmatrix} D_{11} & \vdots & D_{12} \\ \vdots & \ddots & \vdots \\ D_{21} & \vdots & D_{22} \end{bmatrix} \quad (13)$$

Its construction follows a similar pattern given by equations

$$\left. \begin{aligned} [D_{11}] &= 2 \rho \sqrt{mk_1} \cdot \sqrt{F} [I] \\ [D_{12}] &= [D_{21}] = -[D_{11}] \\ [D_{22}] &= 2 \rho \sqrt{mk_1} [\sqrt{R}] \end{aligned} \right\} \quad (14)$$

where an element of $[\sqrt{R}]$ is equal to the sum of the square roots of each term in the corresponding element of [R]. See Table 111.

To exclude degrees of freedom having no mass, the condensed stiffness matrix $[S_c]$ is determined by the static condensation method discussed by Clough and Penzler [11]. $[S_c]$ of size $N \times N$ is calculated from

$$[S_c] = [S_{11}] - [S_{12}] [S_{22}]^{-1} [S_{21}] \quad (15)$$

which reduces to

$$[S_c] = K_1 (F [I] - F^2 [R]^{-1}) \quad (16)$$

The natural frequencies of the system are determinable by solving for the frequencies ω that make the determinant

$$\left| [S_c] - \omega^2 [M] \right| = 0 \quad (17)$$

This formula is made dimensionless by introducing the natural frequency factor f to define

$$\omega = f \sqrt{K_1 / m} \quad (18)$$

Table III.--Construction of matrices [R] and $[\sqrt{R}]$

$$\begin{aligned}
 [R] &= \\
 &\begin{bmatrix}
 N^F + (N-1)^F + F & ; & -(N-1)^F & & ; & 0 & \cdots \\
 -(N-1)^F & & ; & (N-1)^F + (N-2)^F + F & ; & -(N-2)^F & & ; & 0 & \cdots \\
 0 & & ; & -(N-2)^F & & ; & (N-2)^F + (N-3)^F + F & ; & -(N-2)^F & ; & 0 & \cdots \\
 & & & \ddots & & & \ddots & & & & & \\
 & & & \cdots & 0 & ; & -2^F & ; & 2^F + 1 + F & ; & -1 & \\
 & & & & \cdots & 0 & ; & -1 & & ; & 1^F + 0 + F &
 \end{bmatrix} \\
 [\sqrt{R}] &= \\
 &\begin{bmatrix}
 \sqrt{N^F} + \sqrt{(N-1)^F} + \sqrt{F} & ; & -\sqrt{(N-1)^F} & & ; & 0 & \cdots \\
 -\sqrt{(N-1)^F} & & ; & \sqrt{(N-1)^F} + \sqrt{(N-2)^F} + \sqrt{F} & ; & -\sqrt{(N-2)^F} & & ; & 0 & \cdots \\
 & & & \ddots & & & \ddots & & & & & \\
 & & & \cdots & 0 & ; & -\sqrt{1} & ; & \sqrt{1^F} + \sqrt{0} + \sqrt{F} & & &
 \end{bmatrix}
 \end{aligned}$$

Substituting equations (10), (16), and (18) into (17) gives

$$\left| (F [I] - F^2 [R]^{-1}) - f^2 [I] \right| = 0 \quad (19)$$

of which the smallest solution f_1 yields the first natural frequency ω_1 .

The disturbance vector $\{Y\}$ of size $2N \times 1$ is constructed from real and imaginary components of a sinusoidal displacement of infinite duration. The disturbance occurring only at the bottom makes all except one of the elements in $\{Y\}$ equal zero. $\{Y\}$ is partitioned into the complex zero vector $\{0,0\}$ and a complex sub-vector $\{Y'\}$ both of size $N \times 1$ with

$$\{Y'\} = \begin{Bmatrix} 1,0 \\ 0,0 \\ \vdots \\ 0,0 \end{Bmatrix} \quad (20)$$

where the displacement amplitude is normalized to unity. The complete form of $\{Y\}$ is

$$\{Y\} = \begin{Bmatrix} 0,0 \\ Y' \end{Bmatrix} \quad (21)$$

The response vector $\{X\}$ is the set of complex numbers representing sinusoids associated

with the steady state motion of the degrees of freedom and ultimately results from $\{Y\}$. $\{X\}$ has size $2N \times 1$ and is calculated from

$$\begin{aligned}
 \{X\} &= ([S] - \omega^2 [M] + j\omega [D])^{-1} \\
 &\cdot (N^F K_1 + j\omega 2 \rho \sqrt{m} K_1 \sqrt{N^F}) \{Y\} \quad (22)
 \end{aligned}$$

where j is the imaginary unit. This formula is made dimensionless by combining previous equations to get

$$\begin{aligned}
 \{X\} &= \left(\begin{bmatrix} FI & \cdots & -FI \\ -FI & & R \end{bmatrix} - f^2 \begin{bmatrix} I & \cdots & 0 \\ 0 & & 0 \end{bmatrix} \right. \\
 &\quad \left. + jf 2 \rho \begin{bmatrix} \sqrt{F} I & \cdots & -\sqrt{F} I \\ -\sqrt{F} I & & \sqrt{R} \end{bmatrix} \right)^{-1} \\
 &\cdot (N^F + jf 2 \rho \sqrt{N^F}) \begin{Bmatrix} 0,0 \\ Y' \end{Bmatrix} \quad (23)
 \end{aligned}$$

where expressions FI and $\sqrt{F} I$ represent matrices $F [I]$ and $\sqrt{F} [I]$.

APPLICATION

Overcompression of the bottom container causes stack failure. The maximum compression equals the amplitude of the difference between

sinusoids X_{N+1} and Y occurring at ω_1 as given by $|X_{N+1} - Y|$. Repeating the previous analysis leading to equation (23) with units of acceleration instead of displacement yields the maximum compression $|\ddot{X}_{N+1} - \ddot{Y}|/\omega_1^2$. Multiplying this maximum by the spring rate of the bottom container gives the dynamic Compressive load

$$P_d = \left| \ddot{X}_{N+1} - \ddot{Y} \right| K_1 N^r / \omega_1^2 \quad (24)$$

The total load on the box due to statics and dynamics is $P_d + W \cdot N$. The following is

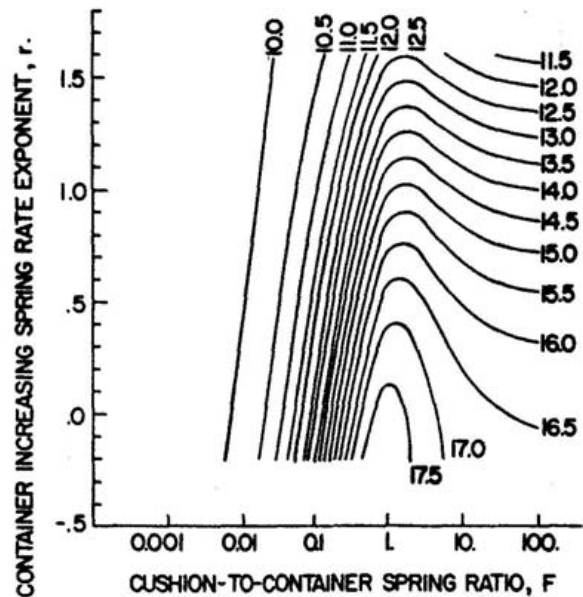
an assessment of a worst-case condition for loading based on the information of Ostrem and Godshall [8] that the envelope of truck vibrations includes the natural frequencies of most unitized loads, and exerts acceleration levels on the order of 0.5 G. The results give the total multiplication of unit weight the bottom container is likely to experience in terms of the dimensionless total compressive loading factor C_t .

$$C_t = \frac{P_d + W \cdot N}{W} = .5 \frac{|\ddot{X}_{N+1} - \ddot{Y}| N^r}{f_1^2 G} + N \quad (25)$$

Values of C_t were calculated for various unit loads with different combinations of r , F , and N . The values $-0.2 \leq r \leq 1.6$ encompass typical values indicated by the repeated loading data. The values $0.001 \leq F \leq 100$ check the effects of relatively very soft to relatively very hard cushions. All calculations assumed $\rho = 0.115$.

Figure 5 shows the effects of r and F on C_t for a four-tier stack. Static conditions would normally load the bottom container to three times its weight. The results show that the maximum total load during shipping can attain about 16 times the unit weight for the lowest r value found in this study. The cause of dynamic compression shifts around $F = 1$. When $K_c > K_1$ the system is "hard" with the cushions becoming increasingly less effective with higher spring rates. Ultimately, the cushions act as though they were rigid. While changing K_1 or K_c (and thus F) has little effect on C_t , increasing r reduces C_t . With effectively rigid cushions the rate of container deformation with increasing top loads governs the magnitude of dynamic loading.

When $K_c < K_1$ the system is "soft" with the cushions becoming more effective as their



ML83 5396

Figure 5.--Contours of constant load multiplication factors C_t calculated for combinations of r and F in a four-tier unitized load. The calculations assume $\rho = 0.115$.

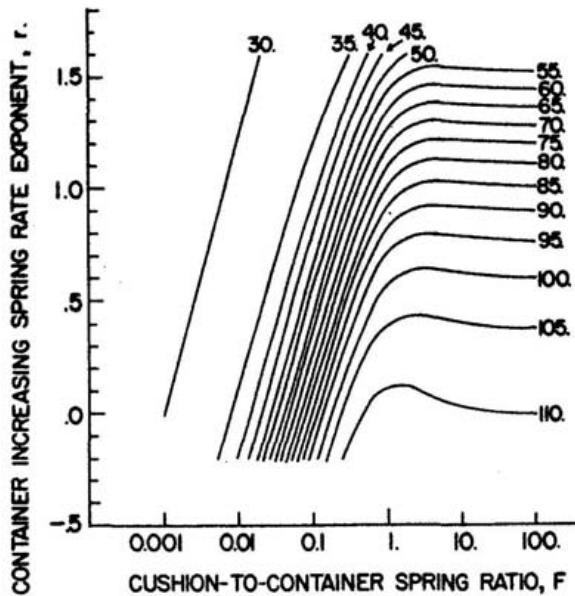
spring rates decrease. While increasing K_1 or reducing K_c reduces C_t , changing r has little effect on C_t . If the cushions have spring rates lower than the containers', the magnitude of loading results primarily from the spring rate of the cushion relative to that of the container.

The shift in the mechanism of dynamic compression makes sense considering how vibration energy gets absorbed throughout the stack. If the system is "hard", the response of each tier is effectively added until the bottom container resists all the action. If the system is "soft", each container absorbs some energy thereby reducing the cumulative response.

The effect of stack height is determinable by comparing previous values of C_t to values

calculated for a ten-tier stack (Fig. 6). The shift between a hard and soft system is again evident and rigid cushions are now possible at lower spring rates. If the unit weight remains unchanged, static conditions would load the bottom tier of a ten-tier stack three times that of a four-tier stack. A representative $C_t = 90$ corresponds to about $C_t = 15$ in

Figure 5, indicating that the expected total load is actually six times more than that of a four-tier stack. Additional tiers are thus more severe not only because they weigh more,



ML83 5397

Figure 6.--Contours of constant load multiplication factors C_c calculated for combinations of r and F in a ten-tier unitized load. The calculations assume $\rho = 0.115$.

but because their weight gets increasingly amplified during shipping.

CONCLUSIONS

The top-to-bottom strength requirements of unitized corrugated containers may exceed the normal static strength requirement depending on the compressive loads caused by transportation vibrations. The spring rates of top-loaded containers and cushions are primary properties determining dynamic loads.

This report proposes new ideas about the progressive deformation of corrugated containers with loading, using a set of dimensionless parameters, r , F , N , ρ , f , and C_c , which reduces the numbers of variables involved with calculating the response. The permanent yielding of material around the top of the box increases its spring rate and superior boxes yield gradually with lower tier position. Inferior boxes that deform excessively during initial loading cause high dynamic loads by equalizing the spring rates of the lower tiers.

Repeated loading experiments provided data on typical spring rates of corrugated containers and plastic bottles. The spring rates increased with greater equilibrium loads due to yielding of material. Flattening the horizontal scoreline, and pressing the bottle caps into the box flaps are primary causes of higher

spring rates with increased loading. As containers are stacked, the spring rate of each tier progressively decreases from the bottom tier to the top tier. Thus, by increasing the rate of changing stiffness in the various tiers using inserts, scoreline stiffness, interior package, etc. the dynamic load can be reduced.

This report also shows how the spring rates of cushions can affect the dynamic loading of containers. Cushions having spring rates lower than those of the containers absorb vibrations and significantly reduce the compressive loads. Extending the concept of a cushion implies that interior packages could be arranged to take advantage of their inherent cushioning ability.

The effects of progressive deformation and of cushions become more pronounced with more tiers. To reduce the dynamic load on the bottom tier you should therefore minimize the number of tiers, make containers that hold their shape with top loading, and softly support the contents using cushions or an effective arrangement of interior packages. It should be noted that excessively soft cushions could bottom-out and result in a damaged product.

ACKNOWLEDGMENT

W. D. Godshall provided data from his own unpublished exploratory investigations.

REFERENCES

1. American Society For Testing and Materials. 1975. Standard methods for vibration testing of shipping containers. D999-75.
2. Godshall, W. D. 1968. Effects of vertical dynamic loading on corrugated fiberboard containers. USDA, For. Serv. Res. Pap. FPL 94, For. Prod. Lab., Madison, Wis.
3. Godshall, W. D. 1971. Frequency response, damping and transmissibility characteristics of top-loaded corrugated containers. USDA For. Serv. Res. Pap. FPL 160, For. Prod. Lab., Madison, Wis.
4. Hatae, M. T. 1976. Packaging design. Shock and Vibration Handbook. McGraw-Hill.
5. Godshall, W. D. 1973. Vibration transmissibility characteristics of corrugated fiberboard. USDA For. Serv. Res. Pap. FPL 211, For. Prod. Lab., Madison, Wis.
6. Urbanik, T. J. 1978. Transportation vibration effects on unitized corrugated containers. USDA For. Serv. Res. Pap. FPL 322, For. Prod. Lab., Madison, Wis.

7. Urbanik, T. J. 1981. A method for determining the effect of transportation vibration on unitized corrugated containers. *The Shock and Vibration Bulletin*. pp. 213-224, May.
8. Ostrem, F. E., and W. D. Godshall. 1978. An assessment of the common carrier shipping environment. USDA For. Serv. Gen. Tech. Rep. FPL 22, For. Prod. Lab., Madison, Wis.
9. Crede, C. E., and J. E. Ruzicka. 1976. Theory of vibration isolation. *Shock and Vibration Handbook*. McGraw-Hill.
10. American Society For Testing and Materials. 1980. Standard method of conditioning paperboard, fiberboard, and paperboard containers for testing. D685-73.
11. Clough, R. W. and J. Penzier. 1975. Dynamics of Structure. McGraw-Hill.

DISCUSSION

Mr. Reed (Naval Surface Weapons Center, Session Chairman): I noticed that your data on the truck and train vibration went up to 100 Hz. That seems contrary to what is more or less standard practice.

Mr. Urbanik: The data are based on a compilation of about four major studies of the rail and truck transportation environments. It is based on the maximum expected acceleration level. There are some more statistically sophisticated presentations of the data, but the approach I used was a simplification that has been documented to smooth out the existing data.